Nuclear Instruments and Methods in Physics Research A294 (1990) 179–192
North-Holland

CALIBRATION OF THE CCFR TARGET CALORIMETER

W.K. SAKUMOTO, P. DE BARBARO, A. BODEK, H.S. BUDD and B.J. KIM
Department of Physics and Astronomy, University of Rochester, Rochester, NY 14627, USA

F.S. MERRITT, M.J. OREGLIA, H. SCHELLMAN * and B.A. SCHUMM **
Enrico Fermi Institute and Department of Physics, University of Chicago, Chicago, IL 60637, USA

K.T. BACHMANN +, R.E. BLAIR ++, C. FOUDAS §, B. KING, W.C. LEFMANN, W.C. LEUNG, S.R. MISHRA, E. OLTMAN **, P.Z. QUINTAS, S.A. RABINOWITZ, F. SCIULLI, W.G. SELIGMAN and M.H. SHAEVITZ
Department of Physics, Columbia University, New York, NY 10027, USA

R.H. BERNSTEIN, F.O. BORCHERDING, H.E. FISK, M.J. LAMM, W. MARSH, K.W. MERRITT, P.A. RAPIDIS and D. YOVANOVITCH
Fermi National Accelerator Laboratory, Batavia, IL 60510, USA

P.H. SANDLER and W.H. SMITH
Physics Department, University of Wisconsin, Madison, WI 53706, USA

Received 12 March 1990

The techniques used to calibrate and monitor the energy response of the CCFR (Lab E) iron–scintillator target calorimeter for a precision measurement of shower energies are described. Measurements on the energy response of the calorimeter to hadrons, electrons, and minimum ionizing muons (from range outs) are presented. The calorimeter's energy response and resolution for hadrons and electrons are obtained using a test beam with energies between 15 and 450 GeV.

1. Introduction

The CCFR (Lab E) neutrino detector is used to study neutrino interactions such as

$$\nu + \text{nucleus} \rightarrow \mu^- + \text{hadrons}, \quad (1)$$

$$\nu + \text{nucleus} \rightarrow \nu + \text{hadrons} \quad (2)$$

using the Fermilab Tevatron quadrupole-triplet neutrino beam. This detector, shown in fig. 1, consists of a total absorption target calorimeter and a muon spectrometer. The target calorimeter is both a neutrino target and a large-area sampling calorimeter that measures the energy of the final-state hadrons. If there are any final-state muons, their kinematics are obtained from both the target calorimeter and the muon spectrometer. The target is used to measure trajectories and the muon spectrometer is used to analyze momenta.

The Fermilab Tevatron quadrupole-triplet neutrino beam is a high-intensity, non-sign-selected wideband beam, with a $\nu : \bar{\nu}$ mix of about 2.5 : 1 and with usable neutrino energies up to 600 GeV. This beam has been used by the CCFR collaboration for two high-statistics neutrino physics experiments: FNAL/E744 (run in 1985) and FNAL/E770 (run in 1987). Because the beam is a wideband neutrino beam, there are no constraints of the measured kinematic quantities: the total visible energy of the final-state hadrons and the 4-momenta of any final-state muons. For precision high-statistics measurements of nucleon-structure functions

* Present address: Fermi National Acceleratory Laboratory, Batavia, IL 60510, USA.
** Present address: Lawrence Berkeley Laboratory, Berkeley, CA 94720, USA.
+ Present address: Widener University, Chester, PA 19013, USA.
++ Present address: Argonne National Laboratory, Argonne, IL 60439, USA.
§ Present address: University of Wisconsin, Madison WI 53706, USA.

0168-9002/90/$03.50 © 1990 – Elsevier Science Publishers B.V. (North-Holland)

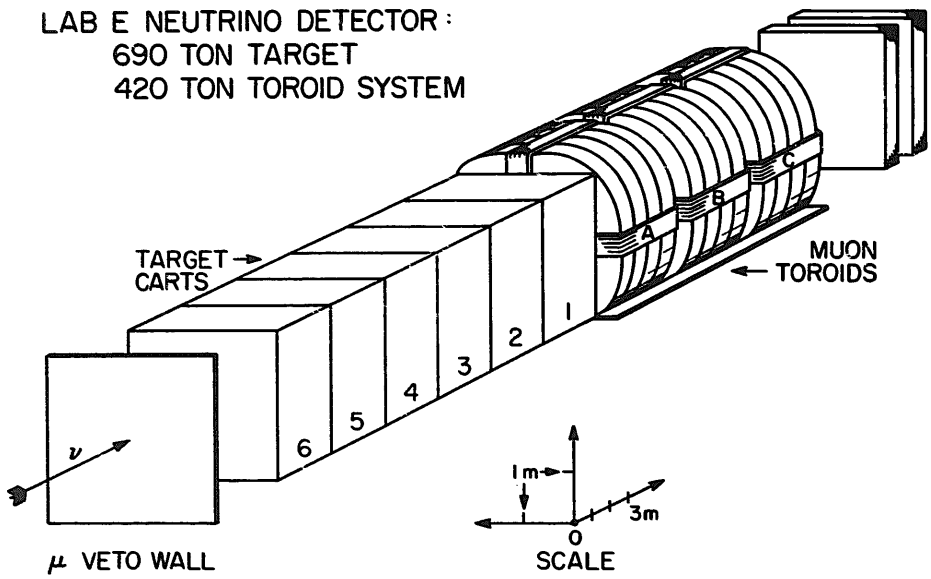

Fig. 1. The Lab E (CCFR) neutrino detector. The target calorimeter consists of six independently movable target carts, numbered 1 through 6 as indicated. The muon spectrometer consists of three toroidal magnet units (A, B and C), and a pair of drift chamber stations at the far downstream end.

or neutral currents, the performance and calibration of the target calorimeter and of the muon spectrometer should be known at the level of a percent or better [1].

Section 2 gives a description of the CCFR target calorimeter. The next section describes the gain calibration and monitoring of the target's calorimetry counters and associated electronics. Section 4 describes the program of total energy calibration with test beams and the associated data analysis. Section 5 gives the results of the calibration.

2. The CCFR target calorimeter

The calorimeter has a mass of 690 tons, a length of 17.7 m, and an average density of 4.2 g/cm^3. This large calorimeter consists of six identical modules called "target carts". Each cart sits on separate a tray which is independently movable. A cart consists of twenty-eight 3 m × 3 m × 5.2 cm steel plates interspersed with fourteen liquid scintillation counters placed every 10.3 cm of steel and seven drift chamber stations placed every

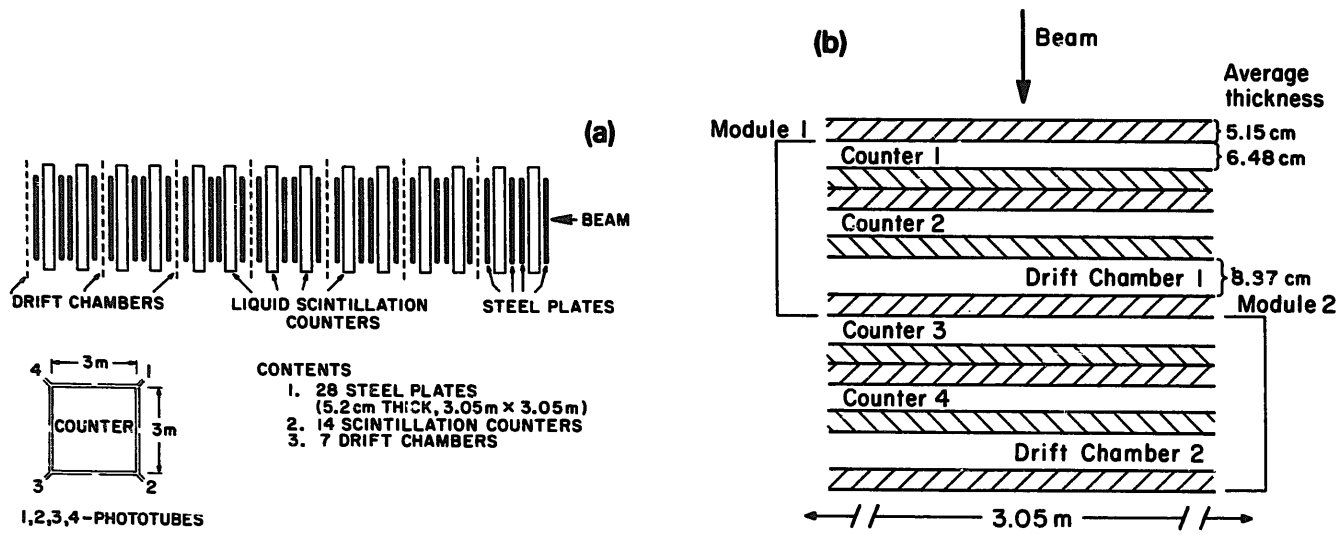

Fig. 2. (a) A view of a calorimeter target cart (not to scale) containing 28 5.2 cm thick steel plates, 14 liquid scintillation counters and 7 drift-chamber stations. A drift chamber station has both an x plane and a y plane. (b) A detailed view of a target cart's components. The mass distribution of these components are given in table 1.

Table 1
Mass distribution of the calorimeter elements. The scintillator oil has a mineral oil base and a hydrogen-to-carbon ratio of 1.8. The Al I-beam braces of the drift chamber are distributed within the drift chamber gas region

Element	Subelement	Length [cm]	Mass [g/cm^2]
Steel plate		5.1532	40.555
Scintillation counter	Scintillator oil	~ 2.54	2.032
	Plexiglas	0.64	0.749
	Water	~ 2.54	2.540
	Mylar and bag	0.76	1.056
Drift chamber	Al Hexcel [3]	2.54	0.857
	Al I-beam braces	–	0.148
	G-10	0.635	1.154
	Cu clad (G-10)	0.0003	0.003
	Chamber gas (50–50 Ar–ethane)	2.858	0.004
	Dead space (air)	~ 2.84	0.003

20.6 cm of steel. Figs. 2a and 2b show the placement and dimensions of these elements within a target cart. Table 1 gives the amount of material presented by these elements.

The scintillation counters have an active volume of 3 m × 3 m × 2.54 cm. This volume is filled with mineral oil doped with a scintillator and a secondary fluor which produces a blue light. The walls of the container consist of 3.175 mm thick plexiglas covered with opaque Marvelguard [2]. To prevent the walls from collapsing, the interior of this container is studded with many plexiglas ribs. To balance the hydrostatic oil pressure, the counter is sandwiched between mylar reinforced polyethylene bags filled with water. These bags press against the adjacent, anchored steel plates. The edges of the container are made of clear, 2.54 cm thick plexiglas. There are 1.27 cm thick BBQ [4,5] doped plastic bars along each edge (with an air gap between) that absorb the blue fluorescence light, reemit light and then transport this light to the four corners of the counter (see fig. 2a). RCA 6342A phototubes are used to read out the light. The sensitivity to a muon traversing through the center of a counter is about 2.5 photoelectrons per phototube.

Analog signals from the phototubes are digitized by the LeCroy 4300 FERA system. This system has features suited for the high-rate environment of the Tevatron quadrupole-triplet wideband neutrino beam: it is fast and buffered (32-event memory; 14 μs for digitizing, buffering, and clearing). The analog-to-digital converters (ADCs) in this system have 11 bits of dynamic range. These ADCs are linear with the gate width set at 240 ns and with the sensitivity at 0.25 pC per ADC count. The leading edge of the gate pulse is timed to arrive 25 ns before the leading edge of the corresponding phototube current pulse; i.e. the integration time is 215 ns. If this gate is shifted to arrive 10 ns later (earlier) than the timing described previously, the digitized phototube signal increases (decreases) by 0.6%.

The analog phototube signals from a single counter are fanned out into channels of different sensitivity and digitized as shown in fig. 3. The pedestals for these ADCs are set at approximately 30 ADC counts. Direct measurements reveal that the LOW channels have at most 0.5% nonlinearity over their full range. The SUPER-LOW channels, which are mixed and attenuated LOW signals (see the caption of fig. 3), have at most 0.2% nonlinearity. The analog sum of the LOWs, the SUM-LO, is slightly nonlinear because the FNAL ES7138 "linear" fan-in modules are about 1.5% nonlinear over the range of the SUM-LO channel. The usage of these channels are described in the next section.

Event time information for each counter is from a discriminated output on the SUM-HI channel. The discriminator produces a 100 ns wide logic pulse if the SUM-HI signal is larger than a quarter of the minimum ionizing level. The timing of this logic pulse is measured using the same time-to-digital converters (TDCs) that are used for the drift chambers. When timing information from all active counters are combined, the event time resolution has an rms of about 2.4 ns. At the Tevatron, there are 18.8 ns between accelerator rf buckets.

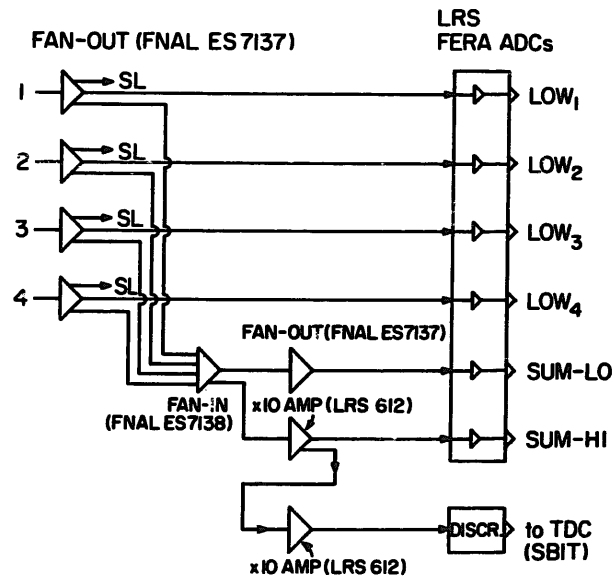

Fig. 3. The readout electronics for a single scintillation counter. The four phototube signals from a counter are labeled as: 1, 2, 3, and 4. The "SL" fan-out output of phototube $N(N = 1, 2, 3, 4)$ from every tenth consecutive counter are mixed, attenuated by a factor of 12, and then digitized by a FERA ADC: this is one of eight SUPER-LOW ADC channels for the phototube N from all counters. The threshold of the SBIT discriminator is set at the quarter of the single minimum ionizing level.

Each drift chamber station has an active area of 3×3 m^2 with 24 horizontal and 24 vertical cells. Each cell is 12.7 cm across, 3 m long, and 1.9 cm thick. It has a left–right ambiguity resolving three-wire cell geometry: a central 0.13 mm diameter field wire with two opposing 0.03 mm diameter sense wires 2 mm from it. The hit information is processed by a buffered, multihit TDC system with 4 ns resolution and a 2 μs live time. This system takes about 12 μs to store an event.

Downstream of the target calorimeter is the 420 ton, magnetized steel, muon spectrometer. It consists of three separate toroidal magnets with drift chamber stations after each magnet and two additional drift chamber stations at the far downstream end. These drift chambers have the same cell size as those in the target calorimeter but each cell only has a single sense wire. Each drift-chamber station consists of five pairs of horizontal and vertical planes. There are muon trigger counters after the first two magnets and 3.81 cm thick acrylic scintillation counters every 20 cm of steel. These counters and drift chambers cover an area of 3×3 m^2. The muon momentum resolution is limited by multiple Coulomb scattering in the steel toroids and $\delta(p)/p \simeq 11\%$. The total transverse momentum kick for a longitudinal track is 2.45 GeV/c and the angular resolution over the full length of the spectrometer (17.8 m) is about 0.3 mrad. The angular-resolution part of the momentum resolution becomes comparable with the multiple Coulomb scattering part at a momentum of about 1 TeV/c.

3. Counter gain calibration and monitoring

Shower energy deposited in any scintillation counter is measured by phototubes at its four corners. The analog phototube signals (see fig. 3) are digitized simultaneously by seven ADC channels of differing sensitivity: a SUPER-LOW, four LOWs, a SUM-LO and a SUM-HI. The four LOW channels view each of the four phototubes individually. A SUPER-LOW is essentially an attenuated LOW. The SUM-LO, HI channels are analog sums of the four LOWs. This collection of 11-bit ADCs with various levels of input gain is equivalent to a single 19-bit SUM-HI channel.

Typically, a minimum ionizing muon that passes through the center of a counter yields 80 ADC counts in the SUM-HI ADC channel, 8 ADC counts in the SUM-LO ADC channel, 2 ADC counts in a LOW ADC channel, and 0.2 ADC counts in a SUPER-LOW ADC channel. The purpose of the SUM-HI channel is to observe minimum ionizing muons clearly. It is used to normalize the positional energy response variation of a counter over its active area and to normalize counter-to-counter gain variations. We call this the "muon calibration". The purpose of the SUM-LO channel is to accurately relate the minimum ionizing muon signal measured in a SUM-HI channel to the corresponding LOW channels. The SUM-LO, HI channels are only used for calibration purposes. The LOW and SUPER-LOW channels are used for calorimetry after counter gain variations are removed via the muon calibration. The SUPER-LOW channel is used only when a LOW channel saturates. One or two LOW channels can saturate when a hadron showers near a phototube or when an energetic hadron in excess of 400 GeV showers near the center of the calorimeter.

The summed energy loss of the SUM-HI channel is used for the muon calibration or relative response normalization of the counters. Its equivalent calculated from the LOW ADC channels is used to measure the shower energies of hadrons and electrons. To convert the energy measured by the four LOW channels of a counter (or by a SUPER-LOW if the LOW has saturated) to that which would be measured by a linear, nonsaturating SUM-LO, HI channel, we use a set of interchannel calibration constants:

$$\text{SUM-LO}_{\text{equiv}} = \sum_{j=1}^{4} \alpha_j \times \text{LOW}_j, \tag{3}$$

$$\text{SUM-HI}_{\text{equiv}} = \beta \times \text{SUM-LO}_{\text{equiv}}. \tag{4}$$

The constants α_j and β are measurable to an accuracy better than 1% because of good overlap in the dynamic range of the channels and because we understand the small nonlinearities in our electronics. ($\alpha_j \sim 0.8$ and $\beta \sim 12$). These constants are fairly stable over time. Major changes occur when malfunctioning electronic modules are replaced. Our analysis software maintains tables of these calibration constants to account for changes over time.

The muon calibration calibrates the response of the counters to a standard signal, the most probable value of the muon $\mathrm{d}E/\mathrm{d}x$ energy loss distribution. Since each counter is uniform over its active area and since all the counters are identical, the $\mathrm{d}E/\mathrm{d}x$ energy deposited by muons as they traverse through any region of any counter is identical. The energy loss at the peak of the $\mathrm{d}E/\mathrm{d}x$ distribution is taken to be the standard unit of energy deposition because the most probable energy loss is expected to be insensitive to the muon momentum while larger energy losses are dependent on it.

The SUM-HI ADC channel is used to observe the intrinsic muon $\mathrm{d}E/\mathrm{d}x$ energy loss distribution. A typical energy loss distribution from a counter is shown in fig. 4. Because of differences in counter gain, the most probable value of the energy loss distribution varies from one counter to another. We estimate the most probable value of these distributions by calculating a "truncated" mean about their peaks. The truncated mean is the mean muon energy loss of the distribution between 20 and 200% of the mean itself. Only cleanly

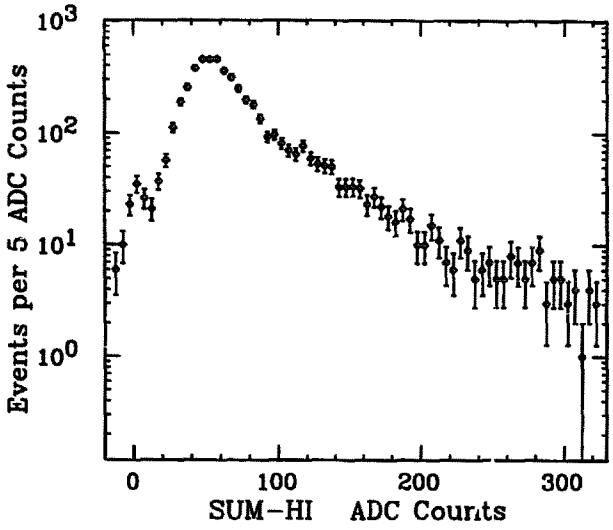

Fig. 4. The muon dE/dx energy loss distribution from the SUM-HI ADC channel of counter number 22. There are many small plastic ribs inside the liquid scintillation counter. Muons that go through these ribs produce the small peak near zero ADC counts.

identified single muons that are momentum analyzed by the toroid spectrometer are used in these distributions. While the upper limit on the mean calculation reduces the sensitivity to the underlying muon momentum distribution, there is still a small dependence. As the muon momentum increases from 10 to 300 GeV/c, the truncated mean increases by 3%. Individual energy loss entries in the distribution that enter the truncated mean calculation are corrected to reduce this muon-momentum dependence. Details are given in appendix A.

Due to the attenuation of light within a counter and differences in its phototube gains, its energy response is not uniform over the active area. The response is not necessarily symmetric among the four phototubes of a counter nor is it necessarily the same among different counters. Muons are used to calibrate this position-dependent energy response because the most probable energy loss of its dE/dx distribution corresponds to a standard unit of energy deposition and because the muon flux associated or produced by the accelerator beam is spread throughout the active area of the counters. The measured energy loss in the SUM-HI ADC channel corresponding to the most probable dE/dx of muons intercepting the counter at the location (x, y) is denoted as $\Delta E_\mu(x, y)$. This response function is extracted for each counter in the following manner. The active area of a counter is binned into a grid of squares, and the energy loss at the dE/dx peak of muons intercepting each bin is measured (via the truncated mean). These discrete measurements over the grid are parameterized to a 15-term ($c_{m,n}$) polynomial:

$$\Delta E_\mu(x, y) = \sum_{m+n=0}^{m+n\le 4} c_{m,n} x^m y^n. \qquad (5)$$

The size of a bin is 23×23 cm^2. Since there are response variations within a bin, we normalize each energy loss entry that goes into a bin's dE/dx distribution to that at the bin center before finding its energy loss at the dE/dx peak. The normalization factor is $\Delta E_\mu(\bar{x}, \bar{y})/\Delta E_\mu(x, y)$, where $(\bar{x}, \bar{y})$ is the bin center and (x, y) is a muon's intercept in the bin. As the extraction process uses the function itself, several iterations are required. For any counter, the function is reasonably flat about a counter's center and steep near its edges (see fig. 5).

SUM-HI equivalent energy measurements (eqs. (3) and (4)), when normalized with the muon calibration function, $\Delta E_\mu(x, y)$, are presumably independent of intercounter and intracounter gain variations. A normalized unit of this SUM-HI energy deposition is called the "Equivalent Particle". The muon calibration function is time dependent because the attenuation length of light in a counter and/or the phototube gains can change. We symbolically denote this time dependence as $\Delta E_\mu(x, y, t)$. Changes in the spatial component of this calibration over time have been found to be modest [6]. Thus we measure the spatial dependence of these functions at a few points in time over a six-month neutrino exposure. We denote the time(s) at which these functions are measured as "$t = 0$", and now discuss how these calibration functions are used at other times.

To calculate energy losses in Equivalent Particle units using $\Delta E_\mu(x, y, t = 0)$, measurements taken at time τ must be adjusted as if they were taken at $t = 0$:

$$\text{SUM-HI}_{\text{equiv}}(t = 0) = \beta(0) \sum_{j=1}^{4} \alpha_j(0) \text{LOW}_j(t = 0). \qquad (6)$$

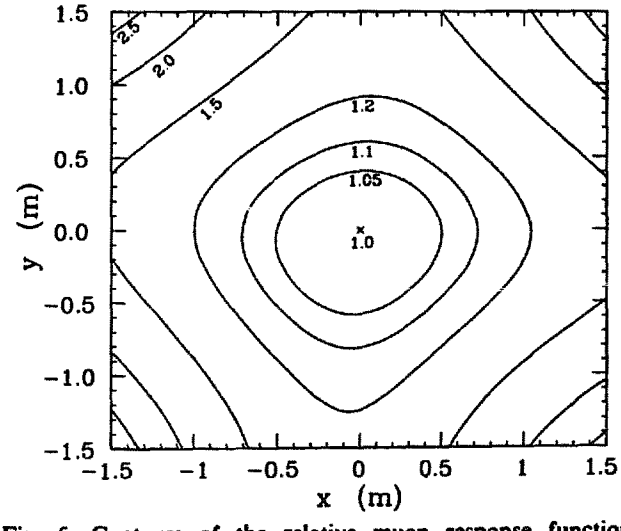

Fig. 5. Contours of the relative muon response function $\Delta E_\mu(x, y)/\Delta E_\mu(0, 0)$ for counter number 33. The (x, y) coordinates are relative to the center of the counter.

Here, $\alpha_j(0)$, $\beta(0)$ are the $t=0$ interchannel calibration constants (eqs. (3) and (4)), and $\mathrm{LOW}_j(t=0)$ is a measurement from a LOW ADC channel taken at time τ with a "$t=\tau$ to $t=0$" gain normalization. In principle, this normalization requires a muon calibration function like $\Delta E_\mu(x, y, t)$ except that a LOW ADC channel is used to measure the muon $\mathrm{d}E/\mathrm{d}x$ instead of the SUM-HI ADC channel. This response function is for a single phototube rather than the sum of a counter's four phototubes. We denote it as $l_j(x, y, t)$, and define it as:

$$\beta(t)\sum_{j=1}^{4}\alpha_j(t)l_j(x, y, t)=\Delta E_\mu(x, y, t), \tag{7}$$

where $\alpha_j(t)$ and $\beta(t)$ are interchannel calibration constants (eqs. (3) and (4)) at time t. To simplify matters, we assume that a counter's time-dependent gain variation is due to phototube gain changes and is therefore decoupled from positional gain variations:

$$l_i(x, y, t)=f_i(x, y)g_i(t). \tag{8}$$

Consequently, the $t=\tau$ to $t=0$ gain normalization of a LOW ADC channel is:

$$\mathrm{LOW}_i(t=0)=\mathrm{LOW}_i(t=\tau)\frac{g_i(0)}{g_i(\tau)}, \tag{9}$$

where $g_i(t)$ are "phototube gains" which are much easier to measure.

Measurements of these phototube gains are made at the center of a counter, where the statistics are largest. Individual phototube gains are extracted from a measurement of muon $\mathrm{d}E/\mathrm{d}x$ at the origin, $\Delta E_\mu(0, 0, t)$, and from measurements of relative gains among the phototubes of a counter. In defining the relative gains, consider an ideal situation where there is shower energy deposited exactly at a counter's center, and where there are no measurement fluctuations from noise or photon statistics. Any differences of measured energy loss among the four LOW ADC channels, LOW_i, would be due to differences in phototube gains. Our relative gain would be defined as $4\mathrm{LOW}_i/\Sigma\mathrm{LOW}_j$, where the sum over j runs over the counter's four phototubes. As there are measurement fluctuations, the relative gains are measured on a statistical basis. We denote these relative gains as $r_i(t)$. The relation between $g_i(t)$ of eqs. (7) and (8) and the measurements are:

$$\beta(t)\sum\alpha_j(t)f_j(0, 0)g_j(t)=\Delta E_\mu(0, 0, t), \tag{10}$$

$$\frac{4f_i(0, 0)g_i(t)}{\sum f_i(0, 0)g_j(t)}=r_i(t), \tag{11}$$

where the sums over j run over a counter's four phototubes. Since values of both $\Delta E_\mu(0, 0, t)$ and $r_i(t)$ vary from one scintillation counter to another, separate measurements are made for each counter, and they are made frequently.

$\Delta E_\mu(0, 0, t)$ is measured using muons that intercept a counter within half a meter of its center. Within this region, the positional dependence of a counter's energy response is fairly flat (see fig. 5). On average, the difference in response relative to the center ranges from -2% to 10%. We normalize the response to the origin using a "bin centering" correction (see discussion beneath eq. (5)). The response function used in the normalization is the one extracted at $t=0$, $\Delta E_\mu(x, y, t=0)$. Since the correction is small, using the $t=0$ response function does not introduce significant errors in this calculation. $\Delta E_\mu(0, 0, t)$ is measurable on a run to run basis to an accuracy of several percent, and it typically decreases by about 10% over the course of a six-month neutrino exposure.

Prior to any extensive data taking, the phototube high voltages were adjusted to equalize the relative gains of a counter's four phototubes. A 1 mCi ^{137}Cs source was positioned at the center of the counter. The high voltages were then adjusted to make the dc anode currents from the four phototube bases equal to within $\pm 25\%$. If the relative gains are ideally balanced by this high voltage adjustment, the four phototubes of a counter output the same signal for excitations at the center. During data taking, the relative gains are extracted from events with hadrons showering within a quarter meter of a counter's center. Even in this small region, the fraction of light produced by shower that is transmitted to a particular phototube depends significantly on the shower's position. At the edges of the region, the fraction of transmitted light differs by about 40% relative to the center. We use a simple model of energy response (cf. $f_i(x, y)$ of eq. (8)) to normalize these differences. A single function is used for all phototubes. It is based on a physical model of light transmission through the counters that uses two attenuation lengths: one for the scintillator oil and other for the light pipes. Over the course of a six-month neutrino exposure, some counter's relative gains drifted by as much as 10%, while others remained stable.

4. Test beam calibration

The CCFR target calorimeter has been absolutely calibrated twice with momentum-analyzed hadron beams. The first calibration run was during the spring of 1984, a year before the E744 neutrino run. The second calibration run was during the winter of 1987, near the end of the E770 neutrino run. Both of these calibration runs were in conjunction with measurements of the muon production rate from hadronic showers [7,8].

The NTW (neutrino test west) beam line at Fermilab is used to calibrate the total energy response of the CCFR target calorimeter. Since it transports beams

directly into the CCFR experimental hall (Lab E), various target carts of the calorimeter are moved horizontally into and out of the beam for calibration without uncabling. Vertically, the beam is pitched onto various locations. This horizontal and vertical adjustment of the beam position on the target carts (± 1 m about the center) permits calibration of not only the center of the calorimeter, but also of its outer regions. This point-to-point calibration gives the residual, positional dependence of the relative normalization of energy to Equivalent Particles described in the previous section. In the calibration of the outer regions of the calorimeter, we expect no significant side leakage of shower particles because the pitch angle is under 25 mrad and because there is at least half a meter of calorimeter remaining to the edge. Since there are ten nuclear interaction lengths to a single target cart, high-energy hadron showers may leak out the back end [7]. Therefore, the target carts are always calibrated as a set: carts 2 and 1, carts 3 and 2 and 1, etc.

The beam configuration where the beam is directed into the center of the leading target cart is designated as *centered beam.* The beam configuration where the beam is directed away from the center of the leading target cart is designated as *pitched beam.*

The NTW beam line transports secondary charged particles produced from interactions between 800 GeV/c primary protons from the Tevatron and a thick, 38 cm aluminum target. Secondary particles are charge and momentum selected by the beam optics. Pions are the dominant component of the secondary beam. For positively charged secondary beams, the proton fraction is about 20% at 100 GeV/c and about 50% at 300 GeV/c. At beam momenta of about 50 GeV/c or less, the electron fraction of the beam is about 10% and increases with decreasing momentum. The kaon fraction is 5% [8] or less. The fraction of muons within the beam aperture ("beam muons") is on the order of a percent and it increases with decreasing momentum. Muons outside the beam aperture ("halo muons") are also transported to the CCFR experimental hall by the fringe fields of the NTW beam-line optics. These halo muons are of either charge and of various momenta.

The momentum of particles in the secondary beam is analyzed by a magnetic spectrometer in an experimental hall (Lab F) just upstream of the CCFR experimental hall. A doublet of Fermilab beam transport EPB dipoles [9] serves as the spectrometer analyzing magnet.

4.1. 1984 calibration run

At the time of this calibration run, the CCFR neutrino detector was being upgraded for the Tevatron run, E744, so it was partially instrumented. Calorimeter target carts 1, 2, and 3 were sufficiently instrumented for calibrations with good systematic cross checks. The calibration of target cart 2 consists of 15, 25, 50 GeV/c centered beam. The calibration of target cart 3 consists of 100, 150, 200, 300, 450 GeV/c centered beam and 100 GeV/c pitched beam onto various locations up to ± 1 m away from the center.

For this calibration run, the NTW beam line selected and transported positively charged particles. Details of the beam-line magnetic spectrometer are given elsewhere [7]. The measured momentum spread σ_p/p of the beam varies from 7% at 15 GeV/c to about 2% at 100 GeV/c or higher. The fraction of beam positrons transmitted by this spectrometer to the calorimeter is large because the amount of material within the beam aperture was small. These positrons are easily identified using only the calorimeter. For the 15 GeV/c centered-beam calibration, a 10 cm lead "filter" was placed within the beam aperture at a position ahead of the spectrometer magnet to remove these positrons.

Energy calibration events were taken on a coincidence between a beam crossing signal and a signal of energy deposition in the CCFR target calorimeter. A small scintillation counter just in front of the analysis magnet provided the beam crossing signal. For the 15 GeV/c calibration, the trigger was just the beam crossing. The beam flux was kept under 1000 particles/s for the centered-beam calibration and under 5000 particles/s for the pitched-beam calibration. Muon calibration events were taken at several occasions during this calibration run (but not simultaneously with the energy calibration points). Halo muons were used for this calibration.

The magnetic field of the spectrometer's analysis magnet was also calibrated. We measured the central field of one of the EPB dipoles as a function of current with an NMR-calibrated Hall probe.

4.2. 1987 calibration run

During this calibration run, the CCFR neutrino detector was fully functional. The calibration of target cart 2 consists of 25, 40, 100 GeV/c centered beam. The calibration of target cart 3 consists of 25, 40, 70, 100, 150, 200 GeV/c centered beam and 40, 70, 100 GeV/c pitched beam onto points (0 m, 1 m) and (-1 m, 1 m) from the center. The calibration of target cart 4 consists of 25, 70, 100, 150, 200 GeV/c centered beam and 40, 100 GeV/c pitched beam onto a single location (-1 m, 1 m) from the center. These specific pitched beam measurements were selected to complement the calibration measurements taken in 1984.

For this calibration run, the NTW beam line was set to select and transport negatively charged particles at the start of data taking, and later switched to select and transport positively charged particles. Due to constraints on the power available for the transport magnets, the beam momentum was limited to 200 GeV/c.

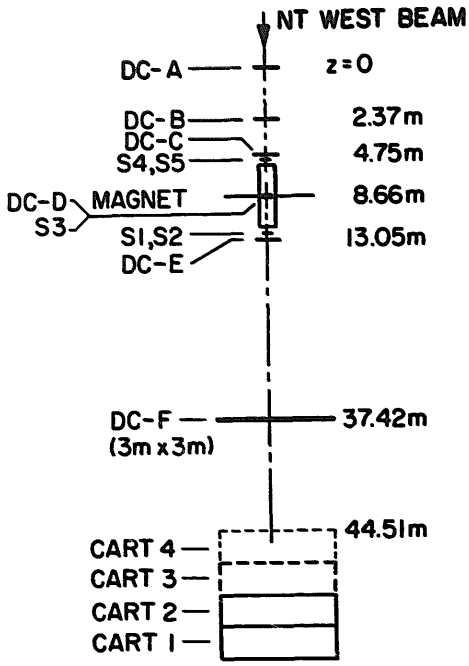

Fig. 6. Plan view of the 1987 test beam spectrometer. It contains two bending magnets, six drift chambers (DC-A through DC-F) and beam-defining counters (S1 through S5). These drift chambers have a mass of about 3 g/cm^2. Not shown are the threshold Cherenkov counters in front of DC-A and behind DC-E.

The layout of the beam-line magnetic spectrometer is shown in fig. 6. It is not exactly the same spectrometer system used in the 1984 calibrations. Although their angular resolutions are similar, the bend angle through the analysis magnet is different: 5 mrad in 1984, and 20 mrad in 1987. In addition, the amount of material within the beam line aperture is much larger. The measured momentum spread (σ_p/p) of the beam is 2% at 25 GeV/c, dips to 1% at 100 GeV/c, and increases to 1.5% at 200 GeV/c. The amount of beam electrons reaching the calorimeter is very small.

Energy calibration events were taken on a coincidence between a beam crossing signal and a signal of energy deposition in the CCFR target calorimeter. A coincidence among the small beam-defining scintillation counters adjacent to the ends of the analysis magnet provided the beam crossing signal. For the 25 GeV/c calibration, the trigger was just the beam crossing. The beam flux was kept well under 1000 particles/s. Muon calibration events were taken simultaneously with the energy calibration. Both beam muons and halo muons from the NTW beam line were used.

4.3. Analysis

A series of analysis cuts, summarized in appendix B, are applied to the energy calibration data to remove unsuitable events. They insure that events are properly reconstructed, that showers are contained longitudinally within the calorimeter, that events contain a single beam particle, and that beam particles pass through the upstream magnetic spectrometer without interacting.

The measurement of shower energy starts from the most upstream counter in the beam and stops at the "shower end". The shower end is the most downstream scintillation counter that has activity in its SBIT discriminator (see fig. 3). These discriminators have a threshold setting corresponding to 25% of the single minimum ionizing level. Shower energies measured by counters within this region are summed to get the total observed energy. Normalized counter energies (in Equivalent Particles) are used in the summation. We denote this total observed energy as "E".

The Equivalent-Particle normalization uses counter gain calibrations obtained from the muon calibration data. For the 1984 data, the normalized counter energy is calculated as it would be for neutrino interaction data (see section 3). For the 1987 data, a simpler but equivalent calculation of the normalized counter energy is used. We measure the muon dE/dx at the shower centroid position, $\Delta E_\mu(\bar{x}, \bar{y}, t)$, and directly normalize the counter energies with it. This is measured with the beam muons of the corresponding energy calibration point. (Beam muons intercept the counters at the shower centroids, and at the same time).

We denote the momentum measured by the upstream magnetic spectrometer as "p" and use GeV units (i.e. $c = 1$). The systematic error in the momentum measurement resulting from uncertainties in the magnetic field of the EPB dipole spectroscopy magnets is 0.5%. Measurements of the central field taken in the 1984 calibration run have a 0.5% error. These measurements agree with those of the EPB dipole reference [9] at the 0.5% level. We infer from this that the current versus magnetic-field excitation curve is uniform from one EPB dipole to another at the 0.5% level. We did not measure the magnetic field during the 1987 calibration run. However, we did calibrate the current and use this in conjunction with a previous measurement [10] of the excitation curve to get the magnetic field.

Since the response of calorimeters to electromagnetic and hadronic showers are in principle different, we separate electrons from the hadrons in the beam. Electrons (positrons) are identified by examining the ratio of the shower energy measured in the three most upstream counters to the total observed energy. Those first three counters cover 1.7 nuclear interaction lengths or 16 radiation lengths. For electrons, the energy ratio is close to 1; for hadrons, it is distributed between 0 and 1 (see fig. 7).

The *pitched beam* calibration reveals a nonlinearity in the digitized signals from phototubes. This is most clearly seen in the 100 GeV *pitched beam* calibration of target carts 3 and 4 taken in 1987. The beam enters the

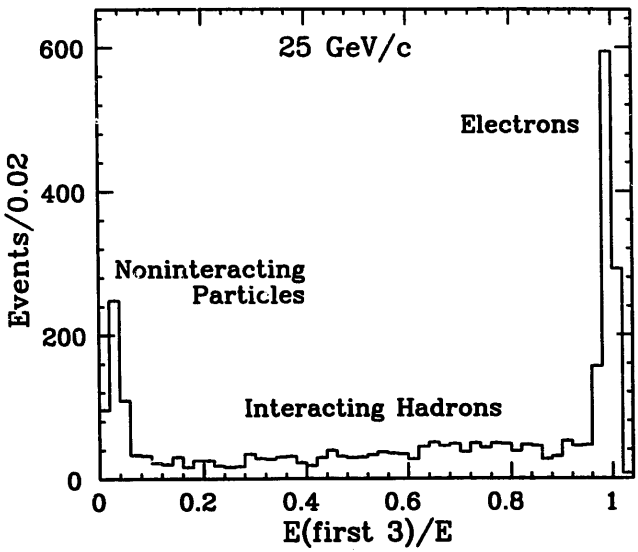

Fig. 7. The distribution of the ratio between the energy in the three most upstream counters and the total observed shower energy. This is from the 1984 centered-beam calibration.

target cart at (−1 m, 1 m) from its center. For this entry point, phototube number 1 (see fig. 2a) sees about 80% of the light from the shower cascade going through a counter. For any counter, the amount of light seen varies considerably because of the large longitudinal fluctuations inherent in hadronic showers. If the digitized responses of the phototubes (LOW_i) are linear, then their asymmetry,

$$ASYM = (LOW_2 + LOW_3 + LOW_4)/LOW_1, \quad (12)$$

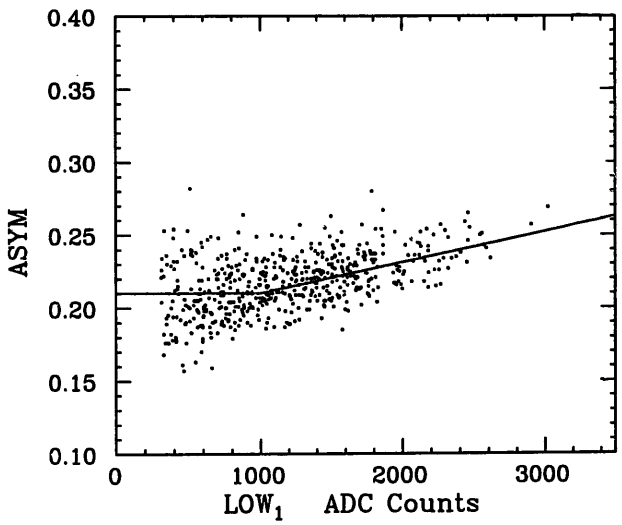

Fig. 8. LOW_1 vs ASYM (eq. (12)) for counter 41 in target cart 3. It is from a 100 GeV/c pitched-beam calibration of 1987. Entries in the $LOW_1 < 300$ ADC count region are not shown. The solid curve is the parametrization of the scatter given in eq. (13). For 300 GeV/c centered-beam hadrons, the mean value of the LOW ADC channels is about 860 ADC counts and the high end tail of the distribution extends to around 1800 ADC counts.

should be constant against LOW_1. This is not observed. Since the readout electronics (LOW, SUPER-LOW ADC channels) are known to be linear at 0.5% or better, the phototube response is presumed to be nonlinear. Fig. 8 shows this nonlinear behavior from a counter in target cart 3 that is about one nuclear interaction length deep. Maximum energy fluctuations are expected in this region where the hadronic cascade just begins. A similar behavior is observed from the 1987 pitched-beam calibration of target cart 4 and from the 1984 pitched-beam calibration of target cart 3.

Analysis of the centered-beam calibration indicate that the total energy response is consistent with being linear up to a beam energy of 200 GeV. From this, we surmise that the phototube response seen in a LOW ADC channel is linear up to a cutoff level of 1000 ADC counts and nonlinear thereafter. Thus the rise in the pitched-beam asymmetry shown in fig. 8 is only from the nonlinear behavior of phototube number 1 because it alone is driven past the cutoff level. We fit this rise to a single-parameter "a" bent line; when $LOW_1 \leq 1000$ ADC counts, ASYM = a, and when $LOW_1 > 1000$ ADC counts:

$$ASYM = a\left[1 + 10^{-4}(LOW_1 - 1000)\right]. \quad (13)$$

This parameterization nominally accounts for the typical behavior of ASYM seen in other counters. It is thus used to correct the nonlinearity of every phototube of all counters; when LOW > 1000 ADC counts:

$$LOW' = LOW\left[1 + 10^{-4}(LOW - 1000)\right], \quad (14)$$

otherwise, there is no correction. The overall effect of this phototube normalization is small. It increases the average total energy of the 100 GeV pitched beam calibration by about 1.5%.

5. Results

5.1. Hadron calibration

The accuracy of the muon calibration affects the shower energy normalization into Equivalent Particle units. For the test beam calibration, the measurement error on the Equivalent Particle unit is 2–3%. This introduces about a 1% error on the total energy measurement of hadron showers.

In hadron showers, backscattered secondaries occasionally escape through the front of the calorimeter. Hadrons that penetrate before interacting should on average have slightly larger total energies because of better containment. To see if this affects the calibration, we measure the total energy for hadrons with no penetration requirement and for hadrons that interact after penetrating beyond the most upstream counter. Penetrating hadrons are required to have a dE/dx loss

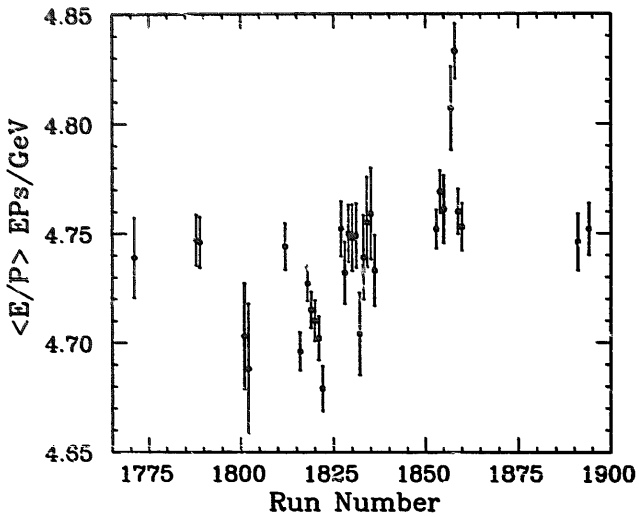

Fig. 9. The energy response of target carts 2, 3 and 4 to 25 to 200 GeV hadrons from the 1987 centered-beam calibration. The total hadron shower energy E is in Equivalent Particle (EP) units. The run numbers corresponding to each target cart calibration are: cart 2 (1770–1810); cart 3 (1811–1851, 1875–1900); cart 4 (1852–1874). Only statistical errors are shown.

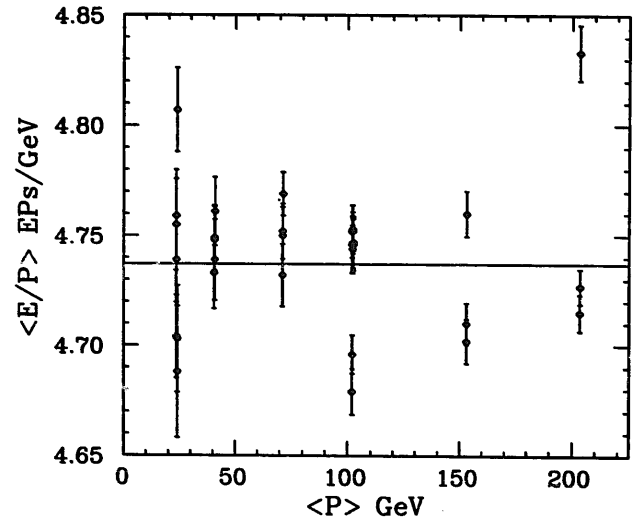

Fig. 10. The energy response of the CCFR calorimeter using hadrons from the 1987 centered-beam calibration. The total hadron shower energy, E, is in Equivalent Particle (EP) units. All the calibration points shown in fig. 9 are in the plot. The horizontal line is the weighted mean (4.737 EPs/GeV) using the statistical error indicated on each point. The fractional rms dispersion about the mean is 0.7%.

consistent with minimum ionizing: under 2.5 Equivalent Particles per counter. We observe no significant differences for 25 or 100 GeV centered-beam calibrations.

The total energy response and resolution of the CCFR calorimeter are obtained from the centered-beam calibrations. For the response, we plot $\langle E/P \rangle$ as a function of $\langle P \rangle$ or of the target cart being calibrated. Here, $\langle \cdots \rangle$ represent means of distributions from the various centered-beam calibrations, "P" is the momentum of a beam particle as measured by the upstream magnetic spectrometer, and "E" is the total energy measured in the calorimeter for that particle. If the energy response is linear, then $\langle E/P \rangle$ is constant. Fig. 9 shows the energy response as a function of the target cart being calibrated. There is no difference in the values of the $\langle E/P \rangle$'s among the identical target carts at the $\pm 1\%$ level.

Fig. 10 is the total energy response as a function of $\langle P \rangle$ obtained from the 1987 centered-beam calibration. Fig. 11 is the total energy response as a function of $\langle P \rangle$ obtained from the 1984 centered-beam calibration. These figures demonstrate that the response between 15 and 450 GeV is linear at the one percent level. There may be a droop in the response at 450 GeV (see fig. 11), but it is at the one percent level. In addition, these figures demonstrate that the total energy response is the same for any experiment performed on the CCFR target calorimeter if the Equivalent Particle counter energy normalization is used.

The calorimeter's total energy distributions are more Poisson in shape than Gaussian, especially at low beam energies. In the parameterization of these distributions, we use a Poisson density extended to accommodate nonintegral arguments:

$$f(x, \bar{x}) = \frac{\bar{x}^x \, e^{-\bar{x}}}{\Gamma(x+1)}, \tag{15}$$

where the arguments are unitless and $\bar{x}$ is the mean. The fit uses two free parameters: a scaling parameter s

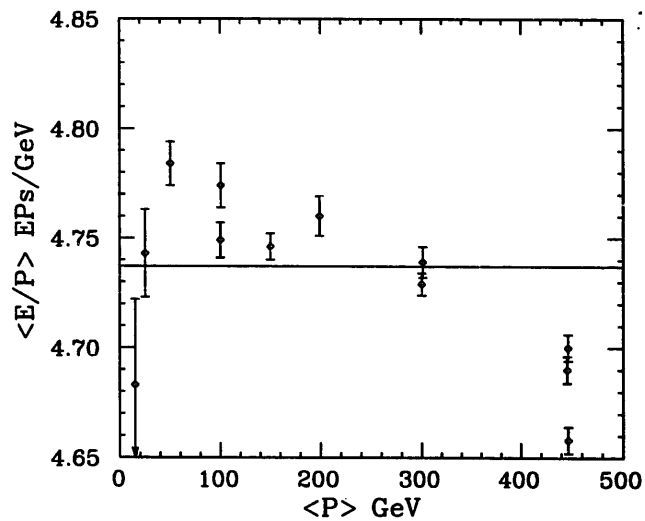

Fig. 11. The energy response using hadrons from the 1984 centered-beam calibration [11]. The shower energy, E, is in Equivalent Particle (EP) units. The horizontal line is the mean value of the 1987 calibration shown in fig. 10. The weighted mean using the statistical error indicated on each point is 4.721 EPs/GeV. The difference is within the 0.5% systematic error from the magnetic-field integrals. The fractional rms dispersion about either mean is 0.8%.

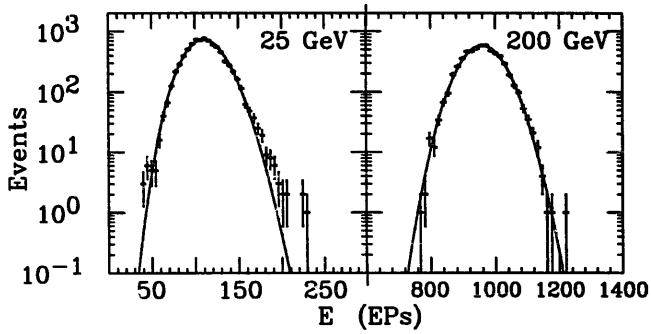

Fig. 12. The total energy distributions of 25 and 200 GeV hadrons from the 1987 centered-beam calibration. The total shower energy E is in Equivalent Particle (EP) units. The solid curves are the Poisson-like parameterizations of the distributions. For the 25 GeV distribution, events in the high-E regions were scanned and found to be acceptable.

that transforms the total energy to the unitless variable $x = E/s$ and the mean. Fig. 12 shows the 25 and 200 GeV total energy distributions from the 1987 centered-beam calibration. The standard deviations and means from these fits, $\sigma = s(\bar{x})^{1/2}$ and $E = s\bar{x}$, are used to obtain the fractional sampling resolution σ/E, which is plotted as a function of the beam momentum (P) in fig. 13. This resolution is parameterized as:

$$\frac{\sigma}{E} = \frac{(0.847 \pm 0.015)}{\sqrt{P}} + \frac{(0.297 \pm 0.115)}{P}, \qquad (16)$$

where P is in GeV. The $1/P$ term is a noise term and it is consistent with independently measured beam-related noise in the calorimetry counters.

The pitched-beam calibrations reveal that the Equivalent Particle normalized total energy response is slightly dependent on position. In these calibrations, the hadron beam is directed to various locations about the center of the calorimeter. This tests how well the muon calibration function, $\Delta E_\mu(x, y, t = 0)$, normalizes the positional energy response variation of the counters to much larger energy depositions from hadron showers. We find that the Equivalent Particle normalized total energy E is lower than expected away from the center of the calorimeter, where the relative muon dE/dx response of the counters:

$$R_\mu(x, y) = \frac{\Delta E_\mu(x, y, t = 0)}{\Delta E_\mu(0, 0, t = 0)} \qquad (17)$$

gets large (see fig. 5). That is, the muon calibration function tends to overcompensate the response of the counters to hadron showers that are outside of the calorimeter's central region. This overcompensation is relative to the hadronic response at the center of the calorimeter, where the response has been determined from the centered-beam calibration. To quantify this overcompensation, we use a parameter which is approximately the ratio of the hadronic shower response at location (x, y) relative to the center:

$$R(x, y) = \frac{\sum \Delta E^i R^i_\mu(x, y)}{\sum \Delta E^i}. \qquad (18)$$

Here, ΔE^i is the Equivalent Particle normalized energy in a counter, $R^i_\mu(x, y)$ is the relative muon response of a counter (eq. (17)), and the sums run over all counters containing the shower. Fig. 14 gives the fractional deviation of the total energy from what is expected, $\delta E/E$,

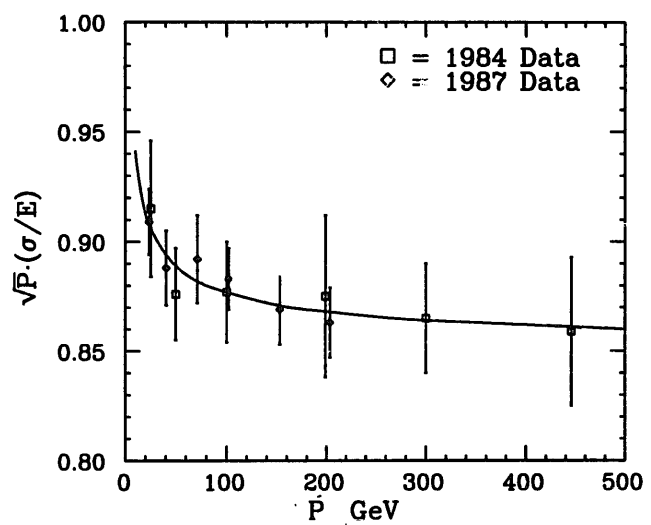

Fig. 13. The hadron shower energy resolution of the CCFR calorimeter from 25 to 450 GeV centered-beam calibrations. The curve is the parameterization given by eq. (16).

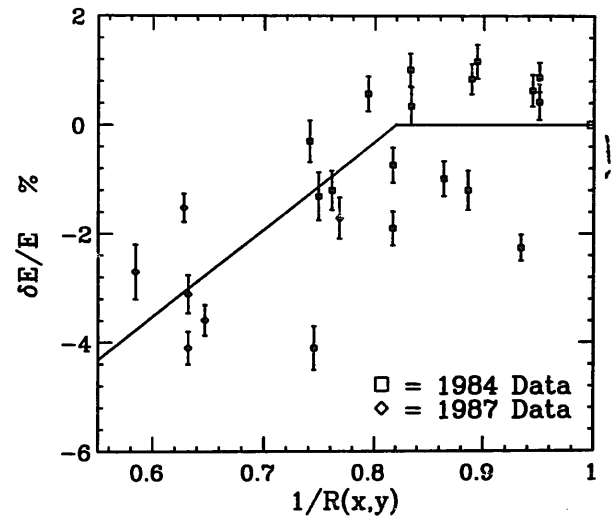

Fig. 14. The fractional deviation of the total hadron energy measured by the calorimeter from that which is expected [12] as a function of $1/R(x, y)$. Here $R(x, y)$ is the estimated hadronic response of a target cart at location (x, y) relative to its center (see eq. (18)). The bent line is a parameterization of the data given by eq. (19). The distribution of the points about the line is consistent with being Gaussian, and the mean and rms are −0.2% and 1.2%, respectively.

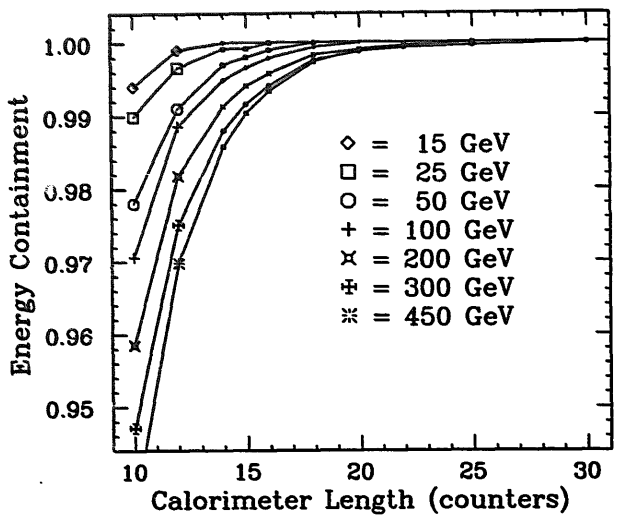

Fig. 15. The fraction of hadronic shower energy contained as a function of the length of the calorimeter. The data are from the 1984 centered-beam calibration. Showers are required to start within the two most upsteam counters in the beam. The errors are about 0.5% at a length of ten counters and decrease to about 0.1% at 20 counters. N counters are $(11.74N - 6.6)$ cm of steel equivalent.

as a function of $1/R(x, y)$. We parameterize this with a bent line; when $R(x, y) > 0.82^{-1}$:

$$\frac{\delta E}{E} = 0.16\left(\frac{1}{R(x, y)} - 0.82\right), \tag{19}$$

otherwise the deviation is zero. This normalizes the residual position dependence of the total energy response for showers away from the center of the calorimeter to that at its center.

With this final normalization, the hadronic energy response of the calorimeter is uniform with position and linear at the $\pm 1\%$ level. The hadronic energy response is thus represented by single number, the calibration constant between Equivalent Particles (EPs) and GeV: 4.730 ± 0.018 EPs per GeV [13]. Here, results from the 1984 and 1987 centered beam hadron calibrations have been combined and the error includes systematic errors.

The energy response and resolution presented are for 100% longitudinal containment of the hadron shower. Partial containment is simulated by removing counters at the end of the calorimeter in the analysis software. The result of this partial containment simulation is shown in fig. 15.

5.2. Electron calibration

From the electron component of the 25 and 50 GeV beams of the 1984 centered beam calibration, we have measured the Equivalent Particle and GeV calibration constant for electron showers. This is for showers that begin in the middle of the two steel plates between counters (see fig. 2a), and it is related to the calibration constant for electromagnetic showers induced by high-energy muons. Such showers are produced uniformly over the two steel plates between counters. While the response of the calorimeter depends on where in the steel the muon-induced shower begins, the response averaged over the two steel plates between the counters should equal the measured electron response.

In addition, we have also extracted the calibration constant for minimum ionizing muons. Neutrino-induced charged-current reactions (eq. (1)) where the final-state muon ranges out in the calorimeter (from the E744 run) are used. To avoid any punchthrough from the shower of the final state hadrons, the muon energy loss is measured in a region sufficiently far from the end of the hadron shower where there is only the muon. Within this region, the total energy deposited by the muon in the calorimetry counters, E, and the path length over which this energy is deposited, L, are measured. The path lengths L of these muons are between 1.1 and 6.1 m of steel equivalent. The muon energy in GeV is calculated using the path length L and range–energy tables [14]. We denote this energy obtained from L and the range–energy tables as P, and they are between 1.5 and 8.7 GeV. The distribution of E/P for the range out muons is shown in fig. 16.

The response of the CCFR target calorimeter to hadronic showers (π), electromagnetic showers (e), and minimum ionizing muons (μ) is different. In terms of the calibration constants between Equivalent Particles (EPs) and GeV, they are:

$$\begin{aligned} \pi &= 4.73 \pm 0.02 \text{ EPs/GeV}, \\ e &= 5.25 \pm 0.10 \text{ EPs/GeV}, \\ \mu &= 6.33 \pm 0.17 \text{ EPs/GeV}, \end{aligned} \tag{20}$$

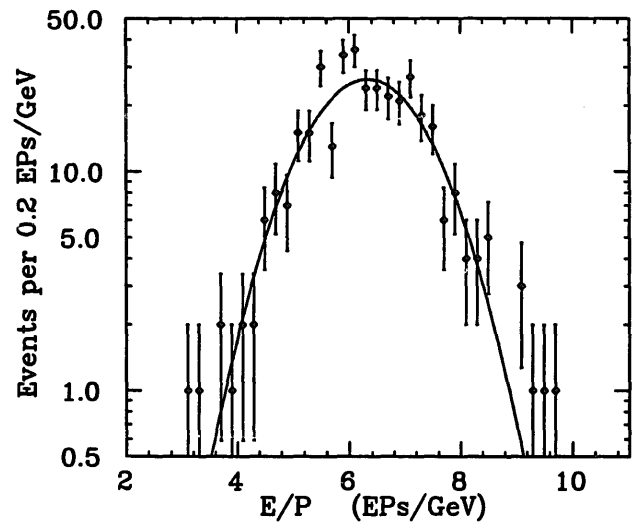

Fig. 16. The E/P distribution for minimum ionizing range out muons. The total energy measured from the calorimetry counters, E, is in Equivalent Particle (EP) units. The muon energy obtained from the path length and the range-energy tables, P, is in GeV. The mean and rms of the distribution are 6.33 and 1.04 EPs/GeV, respectively. The curve is a Gaussian parameterization of the data.

where errors include both statistical and (dominant) systematic errors. The hadronic energy resolution is given by eq. (16). For electromagnetic showers, the resolution is $\sigma_e/E \simeq 0.60/\sqrt{E[\mathrm{GeV}]}$. For the minimum ionizing, range out muons, the resolution is $\sigma_\mu/E \simeq 0.17$.

6. Summary

The energy calibration of the CCFR target calorimeter consists of the relative gain normalization among the scintillation counters with muons and the measurement of its energy response and resolution with a test beam. The hadronic energy response and resolution has been measured for beam energies between 15 and 450 GeV. The level of error on our knowledge of the response is 1%. There are no differences in response among the target carts of the calorimeter that were tested. This is expected because the six component target carts of the calorimeter are identical. In addition, the hadronic energy response and resolution obtained from the two test beam calibrations are consistent with one another. That is, the energy calibration is the same and can be used without adjustment for the two neutrino data runs, E744 and E770, which were taken between the two test beam calibrations.

We have measured the energy response and resolution for 25 and 50 GeV electrons and we have measured the energy response of low-energy (less than 9 GeV) minimum ionizing muons. Their response is different from that of hadrons and we find that the e/π and μ/π ratios are 1.11 and 1.34, respectively.

Acknowledgements

We gratefully acknowledge the contributions of Jean Birkenmaier and Ken Gray for their invaluable technical assistance. We also thank the Fermilab staff, especially the Experimental Areas personnel, for their support. In particular, we thank Gordon Koizumi for assistance in the operation of the NTW beam line. This work is supported in part by the U.S. Department of Energy.

Appendix A

Energy definitions

(1) Muon $\mathrm{d}E/\mathrm{d}x$: the truncated mean

The truncated mean is the mean of the muon energy loss distribution between 20 and 200% of the mean. Since the mean's limits are dependent on the mean itself, the truncated mean is calculated iteratively. In the calculation, individual energy losses in the distribution, ϵ, are shifted to account for the momentum P dependence of the high end of the energy loss distribution:

$$\frac{\Delta\epsilon}{\epsilon} = 0.00967 \ln\frac{P}{77\ [\mathrm{GeV}/c]}.$$

On averaging, this further reduces the residual muon-momentum dependency of the truncated mean. The truncated mean is about 14% larger than the most probably energy loss. Between the limits of the truncated mean, the rms about the mean is approximately 40% of the truncated mean.

(2) Equivalent Particle energy

The energy loss measured by a scintillation counter expressed in Equivalent Particle units is:

$$\Delta E = \mathrm{SUM\text{-}HI}_{\mathrm{equiv}}/\Delta E_\mu(x, y, t),$$

where $\mathrm{SUM\text{-}HI}_{\mathrm{equiv}}$ is defined by eqs. (3) and (4). Since we use a counter's $t = 0$ muon calibration, $\Delta E_\mu(x, y, t = 0)$, the corresponding $\mathrm{SUM\text{-}HI}_{\mathrm{equiv}}(t = 0)$ from eqs. (6) and (9) is used. The phototube gains, $g_i(t)$, are defined by eqs. (10) and (11), and are obtained from the measured muon $\mathrm{d}E/\mathrm{d}x$ at the center of the counter and the relative gains of the counter. Combining them gives:

$$\Delta E = \frac{\beta(t)\sum\alpha_j(t)\mathrm{LOW}_j(t)G_j(0)/G_j(t)}{\Delta E_\mu(0, 0, t)R_\mu(x, y)},$$

$$G_i(t) = 4\alpha_i(t)r_i(t)/\sum\alpha_j(t)r_j(t),$$

where all sums run over the four phototubes of a counter. $R_\mu(x, y)$ is the relative response of a counter to muons (eq. (17)).

Appendix B

Analysis cuts

(1) Clean beam cuts

Only events consistent with a single beam particle within the upstream magnetic spectrometer are allowed. There must only be a single hit in the TDC viewing the beam crossing signal. Upstream showers and beam associated halo are rejected by requiring only one hit within the large upstream drift chamber (in either the x or y view), and by requiring that its location be consistent with that of the beam position. This drift chamber is DC-F in fig. 6.

(2) Momentum reconstruction

The tails of the reconstructed momentum distribution are removed by applying a $\pm 10\%$ cut about the mean. A $\pm 20\%$ cut is applied if the nominal beam momentum is under 30 GeV/c. During the 1987

calibration, some data were taken while the current to the spectroscopy EPB dipoles was being ramped to its set value. This data is not used.

(3) Longitudinal shower boundaries

We look for shower structure above the single minimum ionizing level that is in time with the event trigger. This structure is established using the SBIT discriminators of the scintillation counters (see fig. 3). These discriminators fire when the energy deposition in a counter is larger than 25% of the minimum ionizing level. The time of arrival of these hits are viewed by the TDCs. If there are no SBIT hits, or if the SBIT hit time of a counter is not within ± 2 rf buckets (18.8 ns per rf bucket) of that for the triggering beam particle, the counter is considered to be inactive. This gives a longitudinal map of the energy deposition which is correlated to the showering beam particle. The ensure shower energy containment, an event is rejected if particles penetrate to within three counters of the end of the calorimeter. Penetrating muons are also rejected by this cut.

(4) Electrons

Define $R3$ as the shower energy in the three most upstream counters divided by the total observed energy (see fig. 7). Events with $R3 \geq 0.96$ are identified as electrons. For the 1984 calibration run, the electron sample has about a 10% hadron contamination. For the 1987 calibration run, the electron sample has more than 80% hadron contamination and is not used.

References

[1] F.-L. Navarria, Nucl. Instr. and Meth. 212 (1983) 125.

[2] Marvelguard EC1A is an opaque, conductive anti-stat (MIL-B-81705), Ludlow Laminating and Coating, Homer, LA, USA.

[3] Hexcel structural panel, Hexcel Corp., Dublin, CA, USA.

[4] P. Lasen et al., Nucl. Instr. and Meth. 185 (1981) 67.

[5] B. Barish et al., IEEE Trans. Nucl. Sci. NS-25 (1978) 532.

[6] The relative muon response function, $\Delta E_\mu(x, y, t)/\Delta E_\mu(0, 0, t)$ changes slowly with time; near the corners, (± 1.3 m, ± 1.3 m), the worst-case counter had changes of $\pm 30\%$ over a six-month neutrino exposure.

[7] F.S. Merritt et al., Nucl. Instr. and Meth. A245 (1986) 27.

[8] P.H. Sandler et al., Hadron Shower Punchthrough and Muon Production by Hadrons for 40, 70, and 100 GeV, Univ. of Wisc., Madison preprint: WISC-EX89-306, to be published in Phys. Rev. D.

[9] R. Juhala, Fermilab TM-434 (1973).

[10] Ref. [9], Second Group, table I, appendix B.

[11] For the 15 GeV calibration, an additional 2% normalization error must be included in the statistical error shown. This is due to a muon normalization uncertainty from infrequent muon calibrations and a malfunctioning scintillation counter (counter 26 at shower maximum). The 150 GeV, one of the 300 GeV, and two of the 450 GeV points are measurements at higher beam intensities of about 60000 particles per six second spill.

[12] For the 1984 calibration points, the beam momentum is 100 GeV. The expected energy is the average total energy of beam into the center of target cart 3. For the 1987 calibration, the expected energy is based on the beam momentum and the total energy conversion of 4.737 Equivalent Particles per GeV.

[13] Note that the definition of an Equivalent Particle is based on the truncated mean estimate (see appendix A) of the most probable muon energy loss of a counter. As this truncated mean is about 14% larger than the true most probable energy loss, the corresponding calibration constant between Equivalent Particles based on the true most probable muon energy loss and GeV is about 5.4 (= 4.73 $\times$ 1.14).

[14] G. Koizumi, Fermilab TM-786 (1978). In determining the muon energy from the energy–range tables, we have used 11.49 cm of Fe equivalent as the path length of iron between the calorimetry counters.